

Conformally coating vertically aligned carbon nanotube arrays using thermal decomposition of iron pentacarbonyl

Owen Hildreth, Baratunde Cola, Samuel Graham, and C. P. Wong

Citation: *J. Vac. Sci. Technol. B* **30**, 03D101 (2012); doi: 10.1116/1.3692724

View online: <http://dx.doi.org/10.1116/1.3692724>

View Table of Contents: <http://avspublications.org/resource/1/JVTBD9/v30/i3>

Published by the AVS: Science & Technology of Materials, Interfaces, and Processing

Related Articles

Aluminum-doped zinc oxide formed by atomic layer deposition for use as anodes in organic light emitting diodes
J. Vac. Sci. Technol. A **31**, 01A101 (2013)

Thin InAs membranes and GaSb buffer layers on GaAs(001) substrates
J. Vac. Sci. Technol. B **30**, 051202 (2012)

Impact of post-growth thermal annealing and environmental exposure on the unintentional doping of CVD graphene films
J. Vac. Sci. Technol. B **30**, 041213 (2012)

As-Received, Ozone Cleaned and Ar+ Sputtered Surfaces of Hafnium Oxide Grown by Atomic Layer Deposition and Studied by XPS
Surf. Sci. Spectra **18**, 46 (2011)

Effects of showerhead hole structure on the deposition of hydrogenated microcrystalline silicon thin films by vhf PECVD
J. Vac. Sci. Technol. A **30**, 04D113 (2012)

Additional information on *J. Vac. Sci. Technol. B*

Journal Homepage: <http://avspublications.org/jvstb>

Journal Information: http://avspublications.org/jvstb/about/about_the_journal

Top downloads: http://avspublications.org/jvstb/top_20_most_downloaded

Information for Authors: http://avspublications.org/jvstb/authors/information_for_contributors

ADVERTISEMENT

AVS 59th International Symposium & Exhibition
October 28 - November 2, 2012 • Tampa, Florida

 212-248-0200
avsnyc@avs.org
www.avs.org



DIVISION/GROUP PROGRAMS:

- Advanced Surface Engineering
- Applied Surface Science
- Biomaterial Interfaces
- Electronic Materials & Processing
- Magnetic Interfaces & Nanostructures
- Manufacturing Science & Technology
- MEMS & NEMS
- Nanometer-Scale Science & Technology
- Plasma Science & Technology
- Surface Science
- Thin Film
- Vacuum Technology

FOCUS TOPICS:

- Actinides & Rare Earths
- Biofilms & Biofouling: Marine, Medical, Energy
- Biointerphases
- Electron Transport at the Nanoscale
- Energy Frontiers
- Exhibitor Technology Spotlight
- Graphene & Related Materials
- Helium Ion Microscopy
- *InSitu* Microscopy & Spectroscopy
- Nanomanufacturing
- Oxide Heterostructures-Interface Form & Function
- Scanning Probe Microscopy
- Spectroscopic Ellipsometry
- Transparent Conductors & Printable Electronics
- Tribology

Conformally coating vertically aligned carbon nanotube arrays using thermal decomposition of iron pentacarbonyl

Owen Hildreth

Georgia Institute of Technology, School of Materials Science and Engineering, 771 Ferst Drive, Atlanta, Georgia 30332

Baratunde Cola and Samuel Graham

Georgia Institute of Technology, School of Mechanical Engineering, 771 Ferst Drive, Atlanta, Georgia 30332

C. P. Wong^{a)}

Georgia Institute of Technology, School of Materials Science and Engineering, 771 Ferst Drive, Atlanta, Georgia 30332 and The Chinese University of Hong Kong Shatin, Department of Electronics Engineering, Hong Kong

(Received 17 November 2011; accepted 11 February 2012; published 7 March 2012)

Conformally coating vertically aligned carbon nanotubes (v-CNT) with metals or oxides can be difficult because standard line-of-sight deposition methods, such as dc sputter coating and electron-beam evaporation, are hindered by the low mean-free-path within the vertically aligned array. In this work, we present a facile method to conformally coat dense arrays of v-CNTs using thermal decomposition of iron pentacarbonyl at 205 °C and 30 mTorr. The resulting coatings were found to be uniform from top-to-bottom across an entire $1 \times 1 \text{ cm}^2$ array of v-CNTs. The thickness of the deposited coating was found to be 2–3 nm/cycle and the resulting film thickness were found to be $13 \pm 3 \text{ nm}$ after five cycles and $55 \pm 5 \text{ nm}$ after 20 cycles. This process demonstrates that metal organic chemical vapor deposition can be used to fabricate conformal coatings on v-CNTs. © 2012 American Vacuum Society. [<http://dx.doi.org/10.1116/1.3692724>]

I. INTRODUCTION

Vertically aligned arrays of carbon nanotubes (CNTs) present an interesting case study on the challenges of conformally coating nanostructures. Specifically, the low density and high aspect ratio structural properties that make vertically aligned CNTs (v-CNTs) attractive for applications in capacitors,^{1,2} field effect transmitters,^{3–5} and thermal interface materials,⁶ can also make them difficult to coat. The low volumetric density of v-CNTs results in a physically delicate structure that prohibits many standard processes that require immersion, while the low mean-free-path of a vertically aligned CNT array inhibits dc sputter and electron beam deposition methods for all but the outermost layer. Some recent work in atomic layer deposition (ALD) has shown excellent progress towards using ALD to conformally coat v-CNT arrays;⁷ however, overall the process still requires significant optimization and can be challenged by nonuniformities caused by diffusion, low adhesion, and poor nucleation.^{8,9} Other methods to coat CNTs include supercritical CO₂ hydrolysis to form conformal oxides,^{10,11} or hydrogenolysis to attach metallic nanoparticles;¹² however, neither of these methods have been shown to preserve the alignment of v-CNT arrays.

In this paper we demonstrate a facile method to uniformly coat an array of v-CNTs using metal-organic chemical vapor deposition (MOCVD) of thermally decomposed iron pentacarbonyl, Fe(CO)₅, at low pressure. In an MOCVD process, a sample substrate is placed into a reaction chamber that has either heated sidewalls or a heated

stage while an organometallic vapor is introduced along with any carrier and reactant gasses. The organometallic compound then decomposes to form solid metal,¹³ semiconductor,¹⁴ or oxide^{15–17} coating onto the heated sample substrate with structures ranging from quantum dots,¹⁸ nanorods,^{14,17} or continuous films.¹³ The fact that the organometallic precursors are often delivered in a gas phase with the ability to mix a number of organometallic precursors at the same time or sequentially enables the fabrication of high quality, metastable alloy and compound films when processing conditions, such as temperature, reactants, partial pressures, and substrate material type, orientation, and quality, are well controlled. These films have a wide range of uses in light-emitting devices,¹⁹ solid-state semiconductor lasers,²⁰ and more.²¹ Despite the large amount of research on both MOCVD films and carbon nanotubes, there are surprisingly few examples of MOCVD coatings on CNTs in literature; however, recent work by both Tan *et al.* and Obedkova *et al.* show promising progress toward a conformal coating with Tan *et al.* focusing on magnetic iron and iron oxide nanoparticle coatings while Obedkova *et al.* showed that conformal coatings of Co can be fabricated for CNTs with diameters greater than 100 nm and Co “beads” were created for CNTs with diameters below 100 nm.^{22,23}

In our work, low pressure and a heated stage were used in combination with N₂ vacuum purge cycles to increase the conformability of the MOCVD process. These important processing choices insure that only the sample itself was hot enough to decompose the organometallic, thereby limiting decomposition of the organometallic to those molecules that had adsorbed on the CNT surface. We also chose Fe(CO)₅ as our organometallic precursor to form an iron film because

^{a)}Electronic mail: cp.wong@mse.gatech.edu

$\text{Fe}(\text{CO})_5$ is liquid at room temperature, has a high vapor pressure, a relatively low decomposition temperature of 200°C , and is a zerovalent complex.²⁴ The zero valent nature of $\text{Fe}(\text{CO})_5$ is particularly beneficial because it enables the low temperature decomposition to form solid without any oxidation steps nor the use of a reactive plasma to reduce the organometallic. Unfortunately, the Fe film deposited in this experiment is readily oxidized on contact with air; however, the basic principles used could be applied to a number of different noble metal based organometallics to form stable, conformal thin-metal films.

II. EXPERIMENT

The following procedure was utilized to grow and coat the CNTs. A CNT seed layer was prepared by sequentially depositing 10 nm of Al and 2.2 nm of Fe via electron beam evaporation at 3×10^{-6} Torr or less on top of 100 nm of thermally grown SiO_2 in dry O_2 at 1100°C on (100) silicon wafer. A film of v-CNTs is grown in a tube furnace using standard methods²⁵ on a $1 \times 1 \text{ cm}^2$ chip for 15 min at 720°C using C_2H_2 as the carbon source, Ar as the carrier gas and H_2 to control C_2H_2 pyrolysis. $\text{Fe}(\text{CO})_5$ was decomposed to form a conformal coating on the v-CNTs using the setup shown in Fig. 1. First the sample was placed in a flat-bottomed chamber, labeled "C3." Next, the entire Schlenk line and chamber system was flushed three times with N_2 (99.999%, Airgas) with the system pumped down to less than 10 mTorr between each cycle and then filled with N_2 to 650 Torr. 25 mL of $\text{Fe}(\text{CO})_5$ is introduced into chamber C1 and kept at room temperature. The deposition cycles are as follows: Chambers C2 and C3 are pumped down to 30 mTorr, closed off from the Schlenk line and then valve V2, separating chamber C2 from C3, is closed while valve V1 linking chamber C1, containing the $\text{Fe}(\text{CO})_5$, and chamber C2 is opened for 5 s to introduce $\text{Fe}(\text{CO})_5$ vapor into chamber C2; vapor phase $\text{Fe}(\text{CO})_5$ is evidenced by the vigorous bubbling in chamber C1. Valve V2 between chambers C2 and C3 is opened for 15 s to introduce $\text{Fe}(\text{CO})_5$ vapor into chamber C3 and then V2 is closed. A hot plate set at 220°C is then brought into contact with the bottom of chamber C3 until the temperature of the CNT array reached 205°C as measured using a noncontact

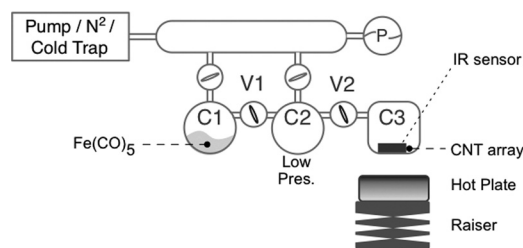


Fig. 1. Schematic of test equipment. A pump and N_2 are connected to a Schlenk line to provide vacuum and N_2 for purging. Chamber C1 holds the $\text{Fe}(\text{CO})_5$ and is connected to the low-pressure chamber, C2, via valve V1. Chamber C3 holds the CNT array and is connected to low-pressure chamber C2 via valve V2. A hot plate set at 220°C is mounted on a raiser to heat the bottom of C3 after $\text{Fe}(\text{CO})_5$ vapor is introduced into C3. The pressure is monitored at the Schlenk line while a noncontact IR sensor monitors the temperature of the CNT array.

IR sensor focused on the CNT array, this took ~ 2 min. At that point, the hotplate is lowered, valve V2 is opened and then chambers C2 and C3 are then purged three times with evacuation to 30 mTorr, flooded to 650 Torr with N_2 . The surface of the v-CNTs is verified to be at room temperature using the IR sensor. The overall deposition cycle is repeated until the desired thickness is achieved. In this work we ran 5 and 20 cycles to show the range and conformability for both thin and thick films.

All samples were imaged using the in-lens detector of a Zeiss LEO 1550 thermally assisted field emission (TFE) scanning electron microscope (SEM) operating at 10–15 kV accelerating voltage and 3–4 mm working distance. The front, center and middle areas Fe coated CNT film were examined in the SEM by removing a section of CNTs using a pair of tweezers. The diameter at the top, middle, and bottom of the CNTs were measured using high magnification and a reduced raster and reduced scan speed to minimize image drift with a total of ~ 200 measurements taken. The spot size of the microscope was around 2–3 nm and the resulting averages were rounded up to 3 nm to reflect this unless the measured standard deviations were larger than 2 nm.

X-ray photoelectron spectroscopy (XPS) of the top surface of the treated v-CNTs was taken to confirm the presence of iron using a Thermo K-Alpha XPS system with a $400 \mu\text{m}$ spot size and utilizing the neutralizing flood gun to minimize charging effects of any air oxidized surface iron.

III. RESULTS AND DISCUSSION

The CNTs were found to have a uniform coating after both 5 and 20 cycles as shown in Fig. 2. The top image shows CNTs near the top of the array with a measured diameter of 15 ± 3 nm before any $\text{Fe}(\text{CO})_5$ deposition. Figures 2(B) and 2(C) show the CNTs near the bottom of the array located in at the center of the $1 \times 1 \text{ cm}^2$ chip to illustrate that the coatings are conformal throughout the entire array; the increased curvature of the CNTs is typical of CNTs near the bottom of the array and is not a result of the $\text{Fe}(\text{CO})_5$ deposition process. The diameter of the Fe coated CNTs was 40 ± 5 nm (13 ± 3 nm of Fe) after five cycles and 125 ± 10 nm (55 ± 5 nm of Fe) after 20 cycles with the variance measured across the sample at five positions near the bottom of the array. The deposition rate was estimated at 2–3 nm/cycle, indicating a relatively thick yet conformal adsorbed $\text{Fe}(\text{CO})_5$ layer prior to decomposition of the $\text{Fe}(\text{CO})_5$ to Fe_{solid} and CO_{gas} .

The conformability achieved by our process stands in sharp contrast to the discrete Fe nanoparticles and larger bead-shaped Co particles achieved by others using MOCVD processes on CNTs.²² Based upon the information available in the experimental methods sections, we can see that cycling and dose control play an important role in enabling conformal coatings on CNTs. In Tan's work using $\text{Fe}(\text{CO})_5$,²² the CNTs were immersed in the $\text{Fe}(\text{CO})_5$ liquid and then dried prior to decomposition under vacuum at 180°C , while in Obedkova's work, a fixed amount of bis-arene-chromium compounds and CNTs were introduced into a sealed chamber and the organometallic compound entirely

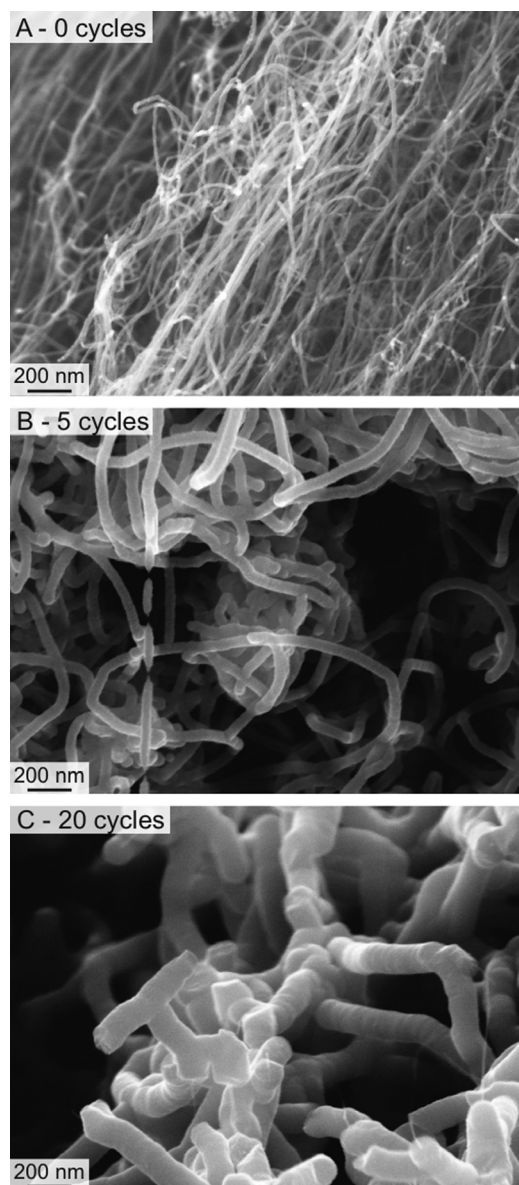


FIG. 2. SEM micrographs of CNTs after (A) 0 cycles, $\text{\O} 15$ nm; (B) 5 cycles, $\text{\O} 40$ nm; (C) 20 cycles, $\text{\O} 125$ nm. The coated CNTs micrographs were taken from the center of the sample near the bottom of the CNT array. The large amount of curvature is typical of CNTs located near the substrate and is not an artifact from the coating process. All scale bars are set to 200 nm as indicated in (A).

decomposed at 400°C .²³ In both cases the amount of organometallic available for decomposition was fixed prior to decomposition and only a single process cycle was used. This stands in sharp contrast to our process in which uses a cycled series of steps that first introduce saturated $\text{Fe}(\text{CO})_5$ vapor at low pressure followed by decomposition of $\text{Fe}(\text{CO})_5$ and then chamber purging. This allows us to slow the deposition rate down to avoid large beading but still deposit a thick Fe layer if desired. In terms of conformability, there are additional benefits of using a carbonyl based complex versus the bis-arene-chromium compounds used by Obedkova *et al.* As it was pointed on in their paper, the decomposition of bis-arene compounds can form organic ligands, which result in beaded structures on CNTs with diameters less than a critical

diameter of 100 nm. The use of $\text{Fe}(\text{CO})_5$, which decomposes directly to Fe_{solid} and CO_{gas} avoids the complication of forming a high surface energy liquid phase and does not bead up on our small diameter CNTs.

XPS was conducted to verify the presence of iron on the carbon nanotube surface as shown in Fig. 3. The survey scan shows the presence of carbon, oxygen, and iron while scans from 700 to 740 eV examine the energies where the Fe 2p binding orbitals are expected.²⁶ This scan shows strong peaks at 710.7 and 724.4 eV, which match up well with the Fe 2p_{1/2} and Fe 2p_{3/2} binding energies of FeO and/or Fe₃O₄ which have binding energies within 0.1 eV of each other and were not distinguished in this study; however, FeO is not thermodynamically stable at room temperature in air and Fe₂O₃ is most likely the composition of the iron carbonyl treated CNTs. This conclusion is further reinforced by the presence of an Fe^{III} satellite peak seen at 718.5 eV. The lack any peaks for Fe_{metal}, which would have been seen at 706.5 and 719.7 eV, is not surprising given that these peaks are not reported in literature in air exposed Fe films until an ion bombardment treatment is used to remove the surface oxidation. Also, some of the thinner depositions could be expected to oxidize completely in air. Unfortunately, transport to the XPS machine in an inert atmosphere was not available and we could not confirm the deposition of pure Fe metal; however, future work will focus on using silver based organometallics to form conformal metal coatings that are stable in air.

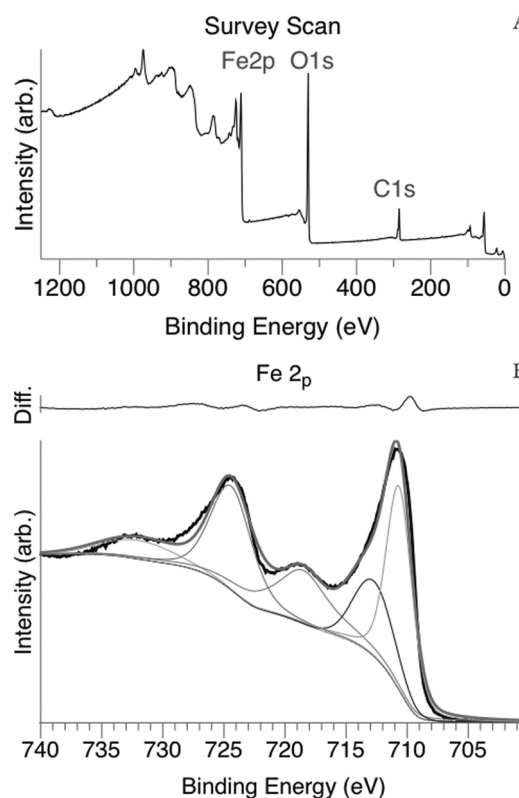


FIG. 3. XPS data showing (A) survey scan and (B) 700–740 eV scan across the Fe 2p energies show the presence of primarily iron oxides on the surface of the iron carbonyl treated CNTs.

IV. SUMMARY AND CONCLUSIONS

In conclusion, we demonstrated a simple method to conformally coat a vertically aligned carbon nanotube array from top-to-bottom and across an entire $1 \times 1 \text{ cm}^2$ sample using thermal decomposition of iron pentacarbonyl by the repeated applications of saturated $\text{Fe}(\text{CO})_5$ vapor at low pressure in combination with discrete heating steps followed by N_2 purging allowed us to control the amount of $\text{Fe}(\text{CO})_5$ deposited. This process was conducted at a relatively low chamber temperature of 220°C with a measured CNT surface temperature of 205°C , resulting in a process that is compatible with low cost glassware and a wide variety of substrates. XPS scans of the treated v-CNT films show the presence of iron oxide with the oxide attributed to the oxidation of the Fe on contact with air. Future tests will utilize silver based organometallics to form an air-stable conformal metal coating on the v-CNTs for applications in thermal interface materials, field emitters, fuel cells, and pseudosuper capacitors.

ACKNOWLEDGMENTS

The authors would like to thank DARPA for their generous funding along with Carlos Alvarez for his assistance.

¹K. H. An, W. S. Kim, Y. S. Park, Y. C. Choi, S. M. Lee, D. C. Chung, D. J. Bae, S. C. Lim, and Y. H. Lee, *Adv. Mater.* **13**, 497 (2001).

²R. H. Baughman, A. A. Zakhidov, and W. A. de Heer, *Science* **297**, 787 (2002).

³J. Bonard, J. P. Salvetat, T. Stockli, L. Forro, and A. Chatelain, *Appl. Phys. A* **69**, 245 (1999).

⁴J. M. Bonard, F. Maier, T. Stockli, A. Chatelain, and W. A. de Heer, *Ultra-microscopy* **73**, 7 (1998).

⁵W. A. d. Heer, A. Châtelain, and D. Ugarte, *Science* **270**, 1179 (1995).

⁶B. A. Cola, J. Xu, C. Cheng, X. Xu, T. S. Fisher, and H. Hu, *J. Appl. Phys.* **101**, 054313 (2007).

⁷S. Kawasaki *et al.*, *Appl. Phys. Lett.* **92**, 1 (2008).

⁸A. Javey *et al.*, *Nat. Mater.* **1**, 241 (2002).

⁹G. Zhan, X. Du, D. M. King, L. F. Hakim, X. Liang, J. A. McCormick, and A. W. Weimer, *J. Am. Ceram. Soc.* **91**, 831 (2008).

¹⁰Z. Liu and B. Han, *Adv. Mater.* **21**, 825 (2009).

¹¹L. Fu, Z. M. Liu, Y. Q. Liu, B. X. Han, J. Q. Wang, P. A. Hu, L. C. Cao, and D. B. Zhu, *Adv. Mater.* **16**, 350 (2004).

¹²Z. Sun, Z. Liu, B. Han, Y. Wang, J. Du, Z. Xie, and G. Han, *Adv. Mater.* **17**, 928 (2005).

¹³J. F. Roeder, T. H. Baum, S. M. Bilodeau, G. T. Stauff, C. Ragaglia, M. W. Russell, and P. C. Van Buskirk, *Adv. Mater. Opt. Electron.* **10**, 145 (2000).

¹⁴A. K. Viswanath, K. Hiruma, M. Yazawa, K. Ogawa, and T. Katsuyama, *Microw. Opt. Technol. Lett.* **7**, 94 (1994).

¹⁵H. W. Kim and N. H. Kim, *Mater. Sci. Forum* **475–479**, 3377 (2005).

¹⁶D. A. Lamb and S. J. C. Irvine, *J. Cryst. Growth* **273**, 111 (2004).

¹⁷G. Perillat-Merceroz, P. H. Jouneau, G. Feuillet, R. Thierry, M. Rosina, and P. Ferret, *J. Phys. Conf. Ser.* **209**, 012034 (2010).

¹⁸T. D. Germann, A. Strittmatter, T. Kettler, K. Posilovic, U. W. Pohl, and D. Bimberg, *J. Cryst. Growth* **298**, 591 (2007).

¹⁹H. G. Kim, T. V. Cuong, M. G. Na, H. K. Kim, H. Y. Kim, J. H. Ryu, and C.-H. Hong, *IEEE Photonic Tech. Lett.* **20**, 1284 (2008).

²⁰Z. Liu, D. Wasserman, S. S. Howard, A. J. Hoffman, C. F. Gmachl, X. Wang, T. Tanbun-Ek, L. Cheng, and F.-S. Choa, *IEEE Photonic Tech. Lett.* **18**, 1347 (2006).

²¹S. Kolluri, Y. Pei, S. Keller, S. P. Denbaars, and U. K. Mishra, *IEEE Electron Device Lett.* **30**, 584 (2009).

²²F. Tan, X. Fan, G. Zhang, and F. Zhang, *Mater. Lett.* **61**, 1805 (2007).

²³A. M. Obedkova, B. S. Kaverina, S. A. Gusevb, A. B. Ezerskiic, N. M. Semenova, A. A. Zaytseva, V. A. Egorova, and G. A. Domracheva, *J. Surf. Invest.-X-Ray* **3**, 554 (2009).

²⁴J. Dewar and H. O. Jones, *Proc. R. Soc. London, Ser. A* **76**, 558 (1905).

²⁵W. Lin, K. Moon, S. Zhang, Y. Ding, J. Shang, M. Chen, and C. Wong, *ACS Nano* **4**, 1716 (2010).

²⁶P. Mills and J. L. Sullivan, *J. Phys. D* **16**, 723 (1983).